

Investigation of Different Oriented 2D Straight Breakwater Under Dynamic Conditions

Mustafa Murat Yavuz¹ , Pınar Sarı Çavdar^{2*} 

¹ İzmir Democracy University, Department of Mechanical Engineering, 35140 İzmir, Türkiye

² İzmir Democracy University, Department of Civil Engineering, 35140 İzmir, Türkiye

*pinar.cavdar@idu.edu.tr

*Orcid No: 0000-0002-1989-4759

Received: 5 January 2023

Accepted: 8 June 2023

DOI: 10.18466/cbayarfbe.1229763

Abstract

There are limited studies in the literature on breakwaters, and studies of the flow structure between the breakwater and the shore are limited. In this study, flow behavior behind a breakwater was investigated for plane-based model. In the examination, straight models at different position angles were used for the breakwater. Dynamic inlet flow was utilized, and the commonly used two-row amplitude wave model was applied. The focus is on the area between the breakwater and the coastline, which is important for the use of breakwaters. $\theta=-8^{\circ}$ results mostly have the lowest total pressure values. The usage of $\theta=+8^{\circ}$ position in placement of straight breakwater gives the most suitable response because of the least dynamic pressure. The results were discussed in detail.

Keywords: Amplitude, breakwater, pressure, wave.

1. Introduction

With the importance given to maritime trade and maritime transport, marinas have gained a lot of popularity. Many studies have been put forward for the development of maritime transport and the design of new ports. Breakwater designs are one of the basic marina structures, and some studies [1-8] have been conducted on their resistance to the pressures which are exposed to them. Dynamic wave motions are complex and some case studies were investigated to understand their physics [9-10]. Different wave models [11] have directly interacted with the breakwater. However, ocean waves move in many directions and are variable. The structure [12] is continuously subjected to forces and moments. The absence or minimal occurrence of damage during the design phase affects the cost analysis of the structure's operation.

The accuracy of the project and the correct construction affect the life of the structure. Hence, structures were inspected and categorized based on whether they were in static or dynamic situations. A case study including wave flumes

[13] were analyzed under irregular waves on a vertical wall. The experimental study have a scale factor of 1:30 compared to a real model and the gained data could be used future designs. Case studies have been done on the effects of slope, and effects of overlapping layer thickness (OLT) and overlapping flow rate (OFV) were [14] investigated. The high variability of waves has necessitated more studies. While the performance of breakwaters [15] has increased with new designs, their structural condition has become more complex.

In the literature, there were few studies on flow behavior for flat breakwaters located in front of the shore. In this study, the flow formed behind a flat breakwater positioned in front of the shore was investigated numerically.

2. Modelling

A numerical model has been created to examine breakwaters operating in time dependent conditions. In Fig. 1, a flat breakwater was modelled in a control area and boundary conditions were shown. The figure also includes different breakwater models.

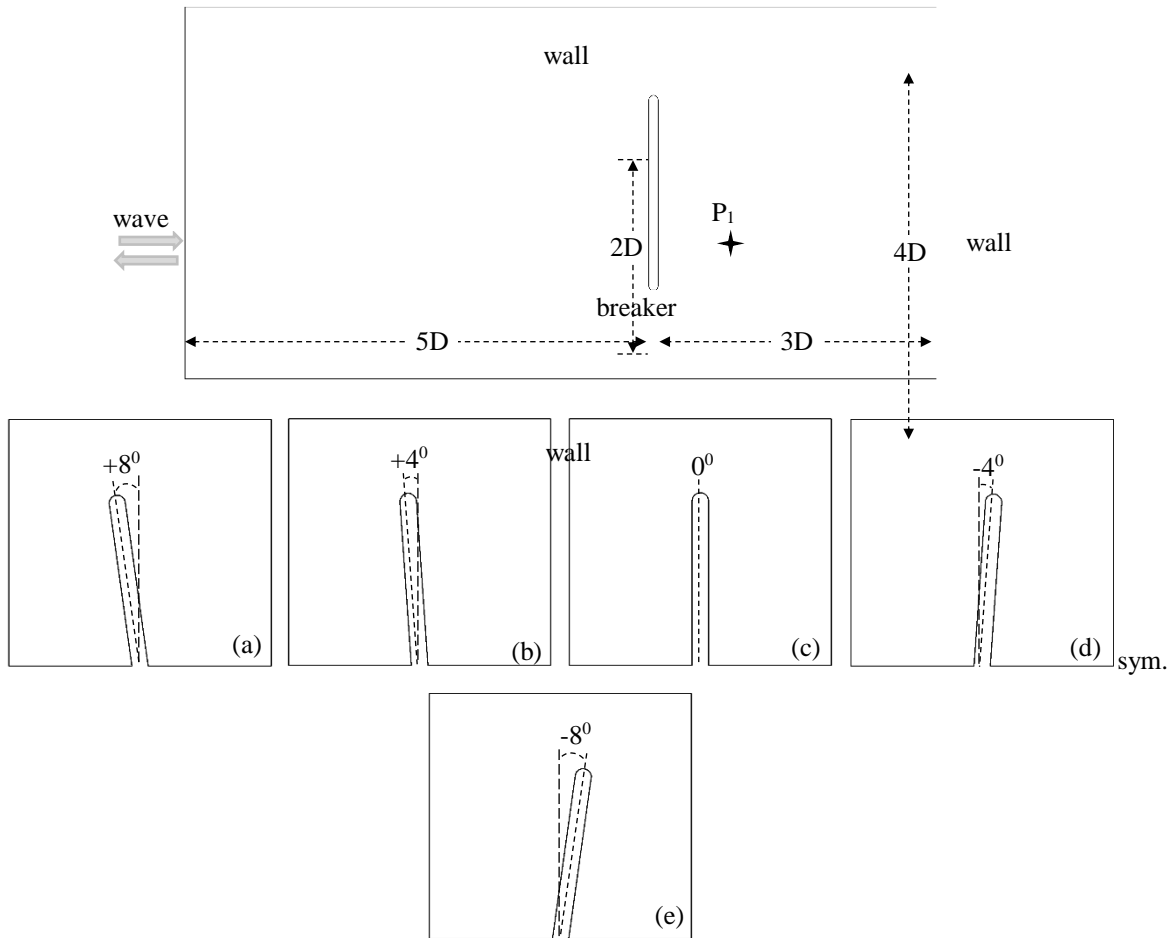


Figure 1. Analysis domain and straight wave breaker models.

As the boundary conditions, the place where the waves entered the control volume was defined as the velocity input. The same place was defined as the outlet to describe the retraction of waves. Breakwater and other edges were defined as wall. Breakwater length ($2D$) was 120 m and all other dimensions were defined according to this length. To measure the wave effects over time behind the breakwater, the P_1 point was defined at a distance of D away from the breaker. The results were obtained at certain time intervals from there. The straight breakwater model was positioned at 5 different angles. k -epsilon, k -omega and RNG (Re-normalization group) turbulence models [16] were generally used in investigations. In the examinations, the standard k -epsilon model was used in turbulence models in order to observe the eddies behind the breakwater structure. The k -epsilon turbulence model is one of the most suitable models among various models in terms of solution sensitivity and resolution time. ANSYS CFD software with default properties was used for simulations.

In Fig. 2, the wave entry velocity to the control volume was given according to time. Water was used as fluid. (density = 998.2 kg/m^3 and dynamic viscosity 0.001003 kg/ms). The analysis was done at 0.002 second intervals for a total of 9 sec.

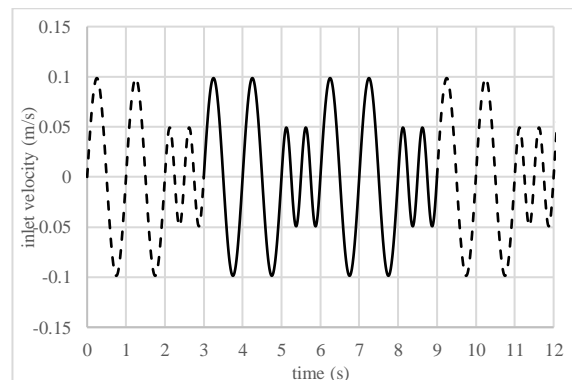


Figure 2. Inlet velocity frequency.

3. Results and Discussion

In Fig. 3, first, the difference between the number of grid elements and the results has been examined in order to see the accuracy and consistency of the numerical solution results. In order to see the results, an analysis was made and instantaneous static pressure on the frontal surface of breaker was considered. Half of the breakwater results was given with respect to symmetry condition. The path length is equal to length of frontal breakwater surface, $D=60$ m. When the results were evaluated, it was suitable for a solution with approximately 56000 elements.

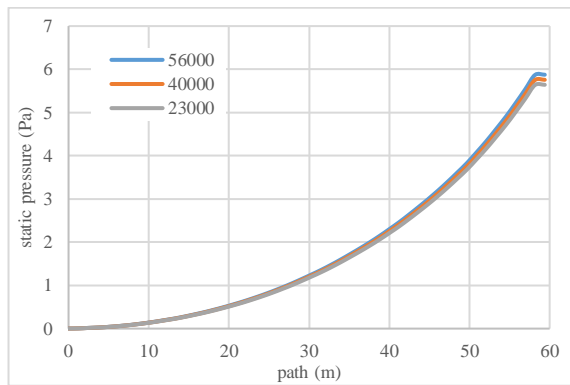


Figure 3. Static pressure on frontal surface of breakwater with respect to number of grid elements.

In order to see the sensitivity in the analysis, 3 different turbulence models were compared in Fig. 4. The k-epsilon turbulence model was used in the rest of the study due to its smaller eddy structure and more pronounced interaction with the breakwater compared to the other two turbulence models.

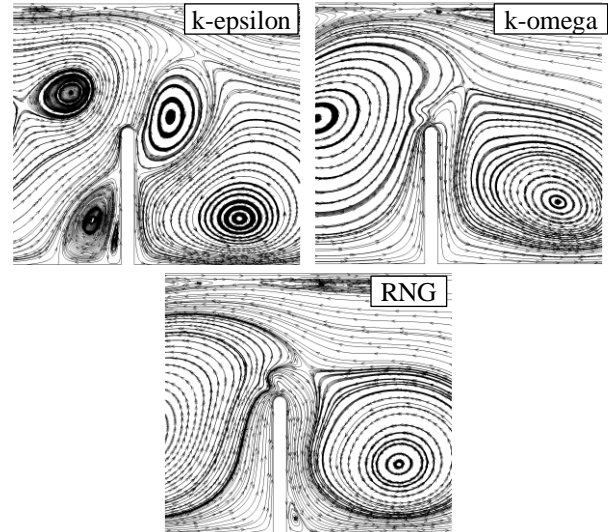
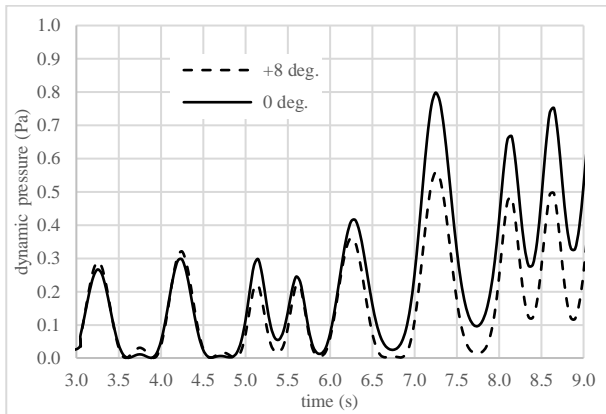


Figure 4. Instantaneous streamline results of different turbulence models at 9 sec.

Dynamic, static and total pressure results were shown at point P_1 over time in Table 1. In the results, the model with the times of low pressure as much as possible was preferred. In the results, mostly the lowest dynamic pressure values were found at $\theta=+8^\circ$. However, the lowest values of the total pressure in general were found at $\theta=-8^\circ$. Considering that the dynamic pressure effect will be more dominant, the $\theta=+8^\circ$ result was accepted as the most ideal according to the other results. $\theta=+8^\circ$ model was compared with $\theta=0^\circ$ straight model.

Table 1. Time dependent pressure values at point P_1 (units in Pa).

time (s)	$\theta=+8^\circ$			$\theta=+4^\circ$			$\theta=0^\circ$			$\theta=-4^\circ$			$\theta=-8^\circ$		
	Dyna.	Static	Total	Dyna.	Static	Total	Dyna.	Static	Total	Dyna.	Static	Total	Dyna.	Static	Total
3	0.027	-42.94	-42.91	0.032	-42.23	-42.19	0.036	-41.67	-41.64	0.025	-43.09	-43.06	0.019	-43.59	-43.57
3.5	0.032	42.03	42.06	0.037	42.87	42.91	0.040	42.05	42.09	0.048	42.52	42.56	0.049	41.97	42.02
4	0.036	-43.57	-43.53	0.055	-43.21	-43.16	0.050	-42.75	-42.70	0.063	-42.70	-42.64	0.070	-42.09	-42.02
4.5	0.028	42.03	42.06	0.062	41.39	41.46	0.024	41.00	41.03	0.030	40.50	40.53	0.030	39.93	39.96
5	0.069	-45.16	-45.09	0.151	-44.66	-44.51	0.112	-44.61	-44.49	0.211	-42.76	-42.55	0.266	-42.73	-42.47
5.5	0.089	-43.38	-43.29	0.080	-45.09	-45.01	0.136	-41.74	-41.61	0.180	-43.22	-43.04	0.261	-42.56	-42.30
6	0.058	-43.32	-43.26	0.093	-43.97	-43.88	0.072	-42.25	-42.18	0.302	-42.47	-42.17	0.723	-41.24	-40.52
6.5	0.075	42.76	42.84	0.345	42.61	42.96	0.164	42.70	42.86	0.712	41.93	42.64	0.827	43.17	44.00
7	0.110	-43.63	-43.52	0.448	-43.75	-43.31	0.250	-43.47	-43.22	0.576	-42.97	-42.39	0.633	-41.66	-41.02
7.5	0.175	42.94	43.11	0.385	42.55	42.93	0.326	42.39	42.71	0.363	42.01	42.37	1.111	41.19	42.30
8	0.242	-43.83	-43.58	0.397	-43.89	-43.49	0.414	-43.55	-43.14	0.438	-43.02	-42.58	1.562	-42.67	-41.10
8.5	0.271	-43.42	-43.14	0.314	-43.43	-43.11	0.476	-42.84	-42.37	0.372	-42.78	-42.41	1.245	-42.37	-41.13
9	0.256	21.01	21.27	0.249	20.96	21.21	0.512	20.71	21.22	0.323	20.44	20.76	0.883	19.90	20.78



In Fig. 4, dynamic pressure values are taken from the P_1 measurement point located behind the breakwater. The average of the solutions stabilized after 2.5 sec. In the vertically used $\theta=0^\circ$ model, the average dynamic pressure is higher and instantaneous results tend to decrease-increase more sharply.

Especially after the 2nd large wave amplitude, this situation seems clearer. The $\theta=+8^\circ$ model yielded the most favorable results, with less sensitivity to wave amplitudes.

Figure 4. Dynamic pressure results at P_1 .

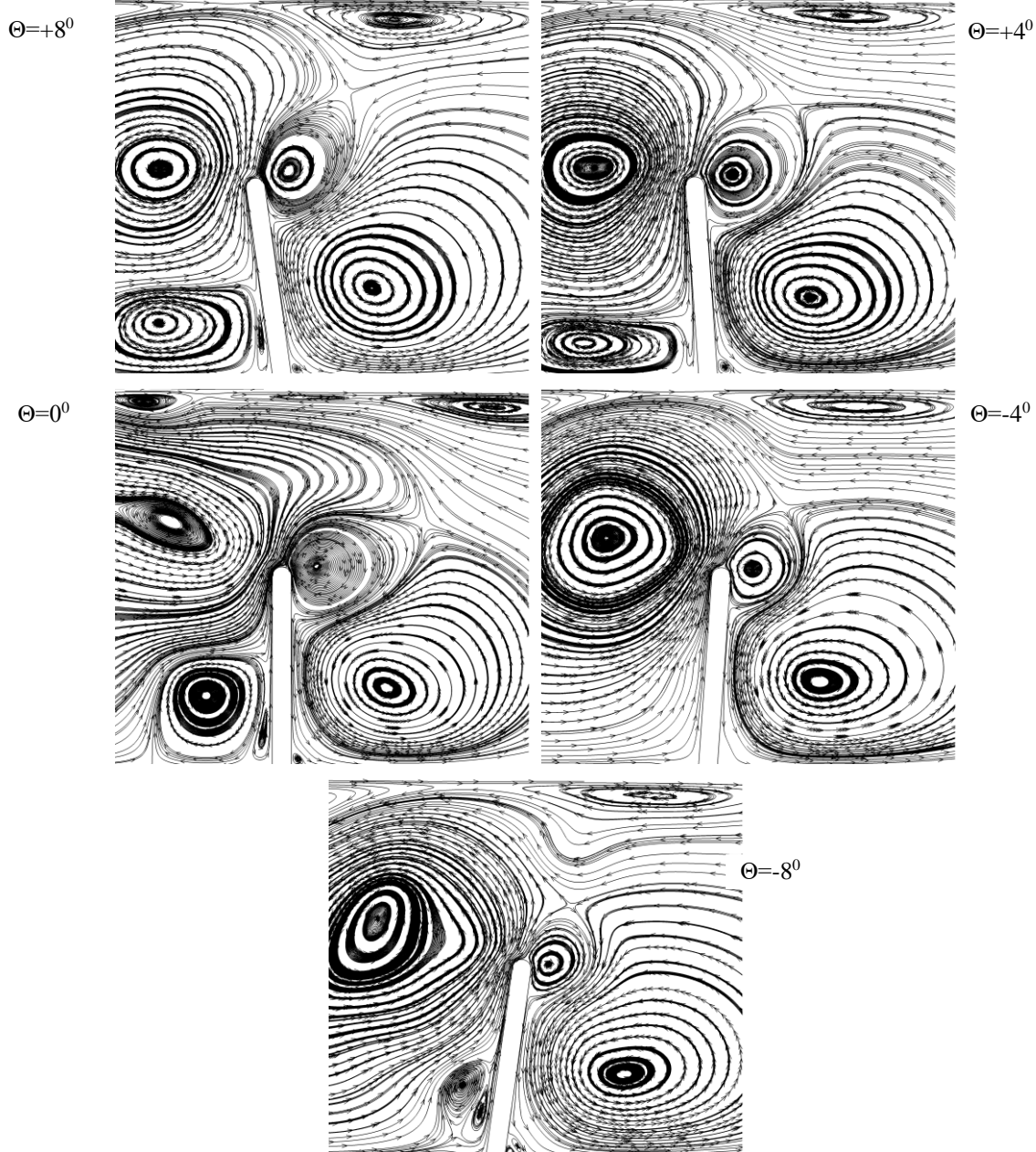


Figure 5. Streamlines of mean velocity at 9 sec.

Average velocity streamlines were shown in Fig. 5. The interaction of the waves with the breakwater and the shore appeared clearly in all results. In the model with $\theta=0^\circ$, a vortex was formed behind the breakwater. Vortex centered $0.5 D$ from the bottom edge and $0.7 D$ from the breakwater. The model results with $\theta=-4^\circ$ were similar. By observing the size of the vortex formed behind the breakwater, the effective distance of breakwater was approximately determined. Only the effective range has increased to $1.6 D$ horizontal length. Similar vortex profile occurred in $\theta=+4^\circ$ and $\theta=+8^\circ$ models, but the effective distance was lower than $1.5 D$. As a result of $\theta=-8^\circ$, the vortex eye has moved predominantly in the vertical direction. The circulation that occurred under the place where the vortex was formed created a flow separation zone.

The effective range of the breakwater has increased to about $2 D$. However, the flow irregularity increased.

The horizontal component of mean velocity profiles was given in Fig. 6. Velocity profiles were shown as the highest H^{++} in the positive direction and the highest L^- in the negative direction. The model in which these profiles formed the least behind the breakwater has occurred as a result of $\theta=+8^\circ$. On the tip of the breakwater, there was a separation zone where a high velocity profile formed. The highest velocity profile in the negative direction mostly formed in the vertical direction from the breakwater tip region. In the results of $\theta=-8^\circ$, the highest positive velocity region appeared to be the most unsuitable profile since it occurs behind the breakwater.

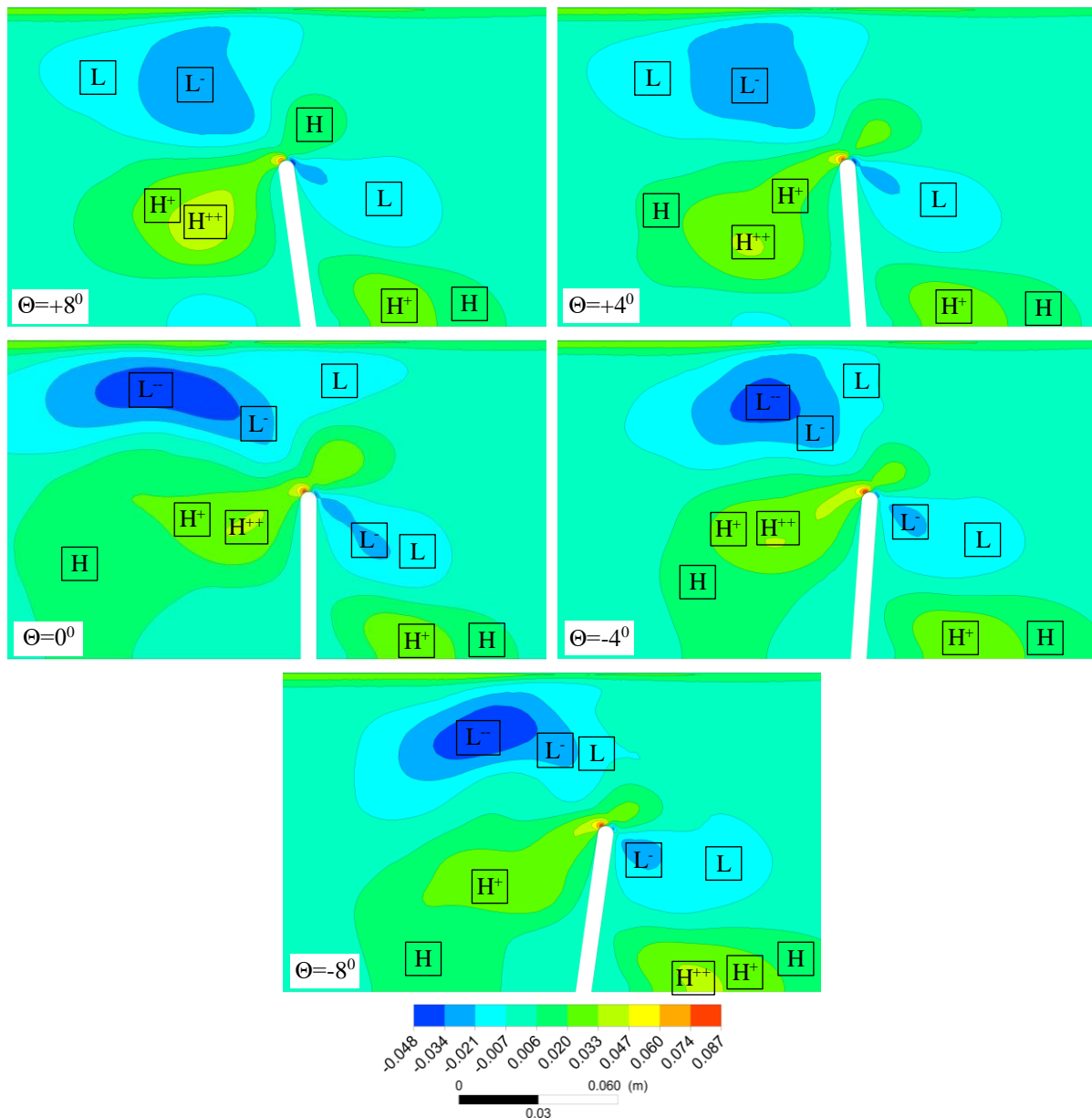


Figure 6. Mean velocity contours at 9 sec. (contour values are in m/s).

4. Conclusion

In this study, straight breakwater models with different position angles were examined numerically. Effect of position angles is given and compared. Time dependent analysis was used, and average results were considered. The results can be summarized;

- The position angle was effective on straight breakwater models and the usage of $\theta=+8^0$ has positive effects
- Most of the least total pressures occurred at $\theta=-8^0$
- The highest velocity profiles formed at the least behind the breakwater has occurred in the result of $\theta=+8^0$

Acknowledgement

This research did not receive any specific grant from funding agencies in the public, commercial, or not-for-profit sectors.

Author's Contributions

M. Murat Yavuz: Obtained and interpreted visuals and tables by doing numerical work.

Pınar Sarı Çavdar: Created the emphasis of the study by writing the literature review and introduction section

Ethics

There are no ethical issues after the publication of this manuscript.

References

- [1]. Miche, R. 1944. Mouvements ondulatoires de la mer in profondeur constante ou décroissante. *Annals des Ponts et Chaussées*; Paris, Vol. 114.
- [2]. Minikin, RR. 1950. Winds, waves and maritime Structures. *Charles Griffin*, London.
- [3]. Ito, Y, Tanimoto, K. 1971. Meandering damages of composite type breakwaters. *Tch.Note of Port and Harbour Res*; Inst., No 112. 20p. (in Japanese)
- [4]. Nagai, S. 1973. Wave forces on structures. *Advances in Hydroscience, Academic Press, New York*; 9: 253–324.
- [5]. Goda, Y. 1974. New wave pressure formulae for composite breakwaters. *Proc. 14th Int.Conf. on Coastal Engineering*; ASCE, 1702–1720.
- [6]. Goda, Y. 1985. Random seas and design of maritime structures. University of Tokyo.
- [7]. Ahrens, JP, Mc Cartney, BL. 1975. Wave period effect on the stability of riprap. *Proc. Civil Engineering in the Ocean III*; 2: 1019-1034.
- [8]. Takahashi, S, Tanimoto, K. 1994. Design and construction of caisson breakwaters – the Japanese experience. *Coastal Engineering*; 22(1–2): 57–77.
- [9]. Van der Meer, JW. 1988. Rock slopes and gravel beaches under wave attack. *Delft University of Technology, Doctoral Thesis*; No. 396, Delft.

[10]. Naimi, S, Özdemir, Z. 2020. Yapılarda yer altı suyuna karşı yapılan koruma sistemlerinin uygulanabilirliği ve güvenliğinin incelenmesi. *AURUM Journal of Engineering Systems and Architecture*; 4(1): 113-133.

[11]. Zhao, XL, Ning, DZ, Zou, QP, Qiao, DS, Cai, SQ. 2019. Hybrid floating breakwater-WEC system: a review. *Ocean Engineering*; 186: 106126.

[12]. Loukogeorgaki, E, Yagci, O, Kabdasli, MS. 2014. 3D Experimental investigation of the structural response and the effectiveness of a moored floating breakwater with flexibly connected modules. *Coastal Engineering*; 91: 164–180

[13]. Huang, J, Chen, G. 2022. Experimental study of wave impact on a vertical wall with overhanging horizontal cantilever slab and structural response analysis. *Ocean Engineering*; 247: 110765.

[14]. Mares-Nasarre, P, Argente, G, Gómez-Martín, ME, Medina, JR. 2019. Overtopping layer thickness and overtopping flow velocity on mound breakwaters. *Coastal Engineering*; 154: 103561.

[15]. Mustapa, MA, Yaakob, OB, Ahmed, YM, Rheem, C, Kohb, KK, Adnana, FA. 2017. Wave energy device and breakwater integration: A review. *Renewable and Sustainable Energy Reviews*; 77: 43–58.

[16]. Dentale, F, Reale, F, Leo, AD, Carratelli, EP. 2018. A CFD approach to rubble mound breakwater design. *International Journal of Naval Architecture and Ocean Engineering*; 10: 644-650.